PERFORMANCE ANALYSIS OF ITERATIVE MIMO-OFDM RECEIVERS UNDER THE PRESENCE OF PHASE NOISE

Steffen Bittner, Ernesto Zimmermann, Wolfgang Rave and Gerhard Fettweis

Vodafone Chair, Technische Universität Dresden, D-01062 Dresden, Germany
Email: {bittner, zimmere, rave, fettweis}@ifn.et.tu-dresden.de

ABSTRACT

The performance of multicarrier transmission in combination with multiple antennas (e.g. MIMO-OFDM) can be drastically degraded due to the existence of RF impairments, e.g. phase noise (PN). In this work we present a performance analysis of iterative receivers where we included the PN statistics in the detection algorithm. The statistical properties of the remaining intercarrier interference (ICI) are analyzed, showing a strong non Gaussian distribution. The impact of this property on the performance is discussed. Finally a modified variance for metric computation is presented leading to an performance improvement.

1. INTRODUCTION

Phase Noise (PN) in communications describes a multiple phase distortion caused by RF imperfections, e.g. imperfect oscillators, during the up- and downconversion. To suppress PN in multiple antenna - multicarrier communications systems (e.g. MIMO-OFDM) the standard correction method is to compensate the common phase error (CPE). However, if higher order modulation are required this can easily become insufficient. We therefore use a PN suppression algorithm initially proposed in [1,2] for single antenna systems which estimates additional spectral components of the PN process apart from the CPE term to mitigate intercarrier interference (ICI) as well. In order to increase performance it is common to perform detector - decoder iterations in a coded MIMO environment. A number of different detection strategies have been investigated in the past, but the influence of RF imperfections is only hardly discussed. However, in an iterative system it is of essential importance to provide the decoder with adequate soft information e.g. log likelihood values (L-values). The L-values are inverse scaled by the AWGN noise, the remaining ICI noise and the multiple antenna interference. In previous contributions [1] - [3] the remaining ICI noise has always be assumed to been Gaussian distributed which is, however, not the case. It will be shown that this is a very crucial fact especially in high SNR regions and if interference cancellation schemes are used where the dominating error term is the remaining ICI. The main contribution of this work is the evaluation and adaptation of interference cancellation techniques affected by PN as well as a comparison with linear MMSE detection [4]. Furthermore we fit a Gaussian curve to the ICI distribution in order to further improve the soft output representation. The remainder of this paper is organized as follows. In Sec. 2 the MIMO-OFDM model disturbed by PN is presented as well as a PN correction algorithm. Sec. 3 describes the modified MIMO detection schemes. The performances are characterized in Sec. 4. Conclusions are drawn in Sec. 5.

Part of this work has been performed in the framework of the IST project IST-4-027756 WINNER II, which is partly funded by the European Union. The authors would like to acknowledge the contributions of their colleagues in WINNER II, although the views expressed are those of the authors and do not necessarily represent the project.

2. FOUNDATIONS

2.1. Phase Noise and MIMO-OFDM Model

We consider MIMO (multiple-input, multiple-output) OFDM transmission with N_{Tx} transmit (Tx), N_{Rx} receive (Rx) antennas and N_C subcarriers. Let $\mathbf{V}$ be a vector of information bits which are encoded by an outer code and interleaved. The resulting code bit stream is partitioned into blocks $\mathbf{X}$ containing $N_{Tx} \cdot N_C \cdot M$ independent binary digits. Here M represents the number of bits per symbol and hence allows to distinguish between 2^M different constellation points. As part of the transmission process, every single block is mapped onto a $N_{Tx} \cdot N_C \times 1$ signal vector $\mathbf{S} = [\mathbf{S}_1, \cdots, \mathbf{S}_l, \cdots, \mathbf{S}_{N_C}]^T$, whose components $\mathbf{S}_l = [S_{l1}, \cdots, S_{ltx}, \cdots, S_{lN_{Tx}}]^T$ denote the $N_{Tx} \times 1$ frequency domain MIMO transmit vectors for each subcarrier. Per antenna the vector is transformed into time domain by performing an inverse fast Fourier transform (IFFT). Before transmission a cyclic prefix (CP) of length N_G is added. This is assumed to be longer than the channel impulse response to eliminate possible intersymbol interference caused by frequency selective channels. The phase noise is modeled by a Brownian motion or Wiener Process resulting in a Lorentzian power density spectrum. However, the PN correction algorithm is also valid for other PN models (e.g. PLL). Furthermore we restrict ourselves to the case of phase noise at the receiver only since transmitter phase noise can be replaced by an effective receiver phase noise as presented in [5].

The phase noise variable at the $(n)^{th}$ sample is related to the previous one as $\phi(n) = \phi(n-1) + w$, where w is a Gaussian distribution random variable, with zero mean and variance $\sigma_w^2 = 4\pi^2 f_c^2 c T_s$. In this notation T_s describes the sample interval and c determines the oscillator quality. Related to the 3dB single side bandwidth $\Delta f_{3\mathrm{dB}}$ of the Lorentzian spectrum, c is given by $c = \Delta f_{3\mathrm{dB}}/(\pi f_c^2)$ [6]. With f_{sub} as the subcarrier spacing of an OFDM system, it is common to use the single relevant performance parameter $\delta_{3\mathrm{dB}}$ as the relative oscillator linewidth with respect to the subcarrier spacing given by $\delta_{3\mathrm{dB}} = \Delta f_{3\mathrm{dB}}/f_{sub}$.

The time domain signal at receive antenna rx in the presence of phase noise can be expressed as:

$$y_{rx}(n) = \sum_{tx=1}^{N_{Tx}} \left(s_{tx}(n) \star h_{rx,tx}(n)\right) e^{j\phi(n)} + \xi_{rx}(n), \quad (1)$$

where $\star$ stands for convolution and $\xi_{rx}(n)$ represents additive white Gaussian noise with variance σ_n^2. In this notation $h_{rx,tx}(n)$ describes the time domain channel impulse response between transmit antenna tx and receive antenna rx. After removing the CP, a discrete Fourier transform is performed per antenna, transforming the received signal back into frequency domain. The overall transmission chain including Fourier transforms is given by the following vector matrix notation:

$$\mathbf{Y} = (\mathbf{F} \otimes \mathbf{I}_{Rx})\mathbf{\Psi}\boldsymbol{\upsilon}\Big(\mathbf{h}\mathbf{\Theta}(\mathbf{F}^{-1} \otimes \mathbf{I}_{Tx})\mathbf{S} + \boldsymbol{\xi}\Big) \quad (2)$$

where uppercase letters describe frequency domain and lowercase letters time domain signals. The symbol $\otimes$ denotes the Kronecker Product, $\mathbf{F}$ is the $N_C \times N_C$ Fourier matrix. The cyclic prefix is added by multiplication with the matrix $\mathbf{\Theta}$ and removed by the multiplication with the matrix $\mathbf{\Psi}$. The phase noise process is represented by $\boldsymbol{\upsilon} = \mathrm{diag}(e_0, \cdots, e_{N_{tot}-1}) \otimes \mathbf{I}_{N_{Rx}}$ with $e_n = e^{j\phi(n)}$. Furthermore the channel is given by the matrix $\mathbf{h}$ of channel impulse responses. Performing standard matrix manipulation the received signal in the frequency domain can be written as:

$$\mathbf{Y} = \mathbf{\Upsilon}\mathbf{H}\mathbf{S} + \boldsymbol{\eta} \quad (3)$$

where we applied the fact that the circular block matrix $\mathbf{\Psi}\mathbf{h}\mathbf{\Theta}$ can be diagonalized by the IFFT and FFT operation resulting in the $N_C \cdot N_{Rx} \times N_C \cdot N_{Tx}$ block diagonal matrix $\mathbf{H}$ which is the frequency domain representation of the channel matrix $\mathbf{h}$. Phase noise at the receiver results in intercarrier interference between received symbols during downconversion, which is modeled in base band by the circulant matrix $\mathbf{\Upsilon}$:

$$\mathbf{\Upsilon} = \begin{pmatrix} E_0 & E_{-1} & \cdots & E_{-(N_c-1)} \\ \vdots & \vdots & \ddots & \vdots \\ E_{N_c-1} & E_{N_c-2} & \cdots & E_0 \end{pmatrix} \otimes \mathbf{I}_{Rx} \quad (4)$$

and $E_k = \frac{1}{N_C} \sum_{n=0}^{N_C-1} e^{-j2\pi kn/N_C} e^{j\phi(N_G+n)}$ the frequency domain representation of the phase noise process. The statistical property of the transformed AWGN noise stay the same.

2.2. Iterative Phase Noise Correction

A detailed MIMO-OFDM transmission chain including iterative PN correction is shown in Fig. 1. After an initial correction of the common phase error (CPE) with the help of known pilots [3] and decoding a first estimation of the transmitted symbols is available. However, this estimation is not very reliable in frequency selective channels, since each received symbol is still afflicted by a weighted sum over all other subcarriers. Therefore we will take the idea of joint linear minimum mean square error (LMMSE) estimation of CPE and ICI for every further iteration [1,2]. The key idea of this approach is to estimate higher order phase noise components. In order to obtain a Bayesian estimator for the spectral components E_k up to a certain order u (e.g. $k \in \{-u, \cdots, u\}$) we rewrite Eq. (3) in a vector matrix notation for a subset of $B \geq 2u+1$ equations [4]:

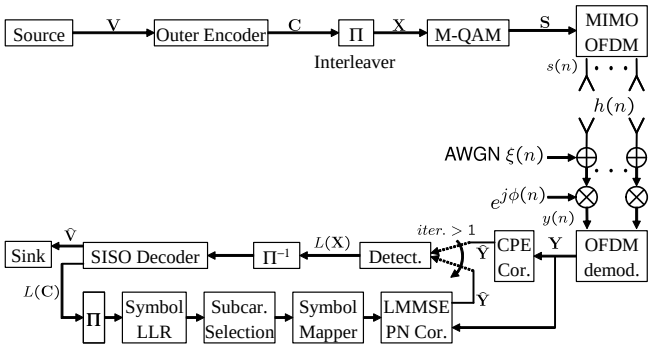

Fig. 1. OFDM transmission in the presence of phase noise with spatial multiplexing and iterative correction.

$$\mathbf{Y} = \mathbf{A} \cdot \mathbf{E} + \boldsymbol{\varepsilon} \quad (5)$$

where $\mathbf{A}$ is a $B \times 2u+1$ matrix containing the products of $\mathbf{H} \cdot \mathbf{S}$. Furthermore, $\mathbf{E}$ is a $2u+1 \times 1$ PN vector and $\boldsymbol{\varepsilon} = \boldsymbol{\zeta}_{ICI} + \boldsymbol{\eta}$ represents the effective noise consisting of remaining ICI noise and AWGN noise. The LMMSE estimate of the vector $\mathbf{E}$ is given by

$$\hat{\mathbf{E}} = \mathbf{M} \cdot \mathbf{Y} \quad (6)$$

with $\mathbf{M} = \mathbf{\Phi}_{\mathbf{EE}}\mathbf{A}^H(\mathbf{A}\mathbf{\Phi}_{\mathbf{EE}}\mathbf{A}^H + \mathbf{\Phi}_{\boldsymbol{\varepsilon\varepsilon}})^{-1}$ and $\mathbf{\Phi}_{\mathbf{EE}}$ and $\mathbf{\Phi}_{\boldsymbol{\varepsilon\varepsilon}}$ representing correlation matrices of the vector of Fourier components $\mathbf{E}$ and the remaining noise terms $\boldsymbol{\varepsilon}$, respectively. The evaluation of the correlation matrices $\mathbf{\Phi}_{\mathbf{EE}}$ and $\mathbf{\Phi}_{\boldsymbol{\varepsilon\varepsilon}}$ can be found in [4, 7]. A modification of remaining ICI variance is described in more details in Section 4. Having obtained the coefficients $\hat{\mathbf{E}}$ the complex conjugate of the Fourier expansion can be used to correct the received signal samples in time domain: $\hat{y}_{rx}(n) = y_{rx}(n)e^{-j\hat{\phi}(n)}$.

3. MIMO DETECTION SCHEMES

The aim of the MIMO detector is to provide soft information to the outer decoder for each bit. This information is based on the modified received signal $\hat{\mathbf{Y}}_l$, the channel state information and the a-priori knowledge ($P[X_{tx,m}]$) from the same outer decoder. In order to increase the readability we drop the subcarrier index l in the following. Using Bayes'theorem and under the assumption of statistically independent bits, the L-value of a certain bit is defined as:

$$L(X_{tx,m}|\hat{\mathbf{R}}) = \ln \frac{\sum_{\mathbf{X}\in\mathbb{X}_{tx,m+1}} p(\hat{\mathbf{R}}|\mathbf{X}) \cdot P[\mathbf{X}]}{\sum_{\mathbf{X}\in\mathbb{X}_{tx,m-1}} p(\hat{\mathbf{R}}|\mathbf{X}) \cdot P[\mathbf{X}]} \tag{7}$$

Using the so called *max*-Log approximation, the L-values from the detector can be approximated by a difference of two maximum operation [8]:

$$\begin{aligned} L(X_{tx,m}|\hat{\mathbf{Y}}) \approx & \max_{\mathbf{X}\in\mathbb{X}_{+1}} \left\{ \frac{-\gamma_{tx}}{\sigma^2_{S_{tx}}} \left\| \hat{\mathbf{Y}} - \mathbf{HS} \right\|^2 + \ln \prod_{tx=1}^{N_{Tx}} \prod_{m=1}^{M} P[X_{tx,m}] \right\} \\ & - \max_{\mathbf{X}\in\mathbb{X}_{-1}} \left\{ \frac{-\gamma_{tx}}{\sigma^2_{S_{tx}}} \left\| \hat{\mathbf{Y}} - \mathbf{HS} \right\|^2 + \ln \prod_{tx=1}^{N_{Tx}} \prod_{m=1}^{M} P[X_{tx,m}] \right\}. \end{aligned} \tag{8}$$

For the implementation of Eq. (8) a lot of MIMO detection strategies are known. The common basis of most of the schemes is the correlation matrix of the transmitted signal $\mathbf{\Phi_{SS}}$ and the correlation matrix of the remaining noise $\mathbf{\Phi_{\epsilon\epsilon}}$. In a coded environment the knowledge of the SINR γ_{tx} at each antenna is of essential importance. Due to the limited space we will give only the solution of the general expression of the SINR for each detection scheme.

3.1. Linear MMSE equalization

A low complexity scheme is an adapted linear MMSE equalization [4]. The solution of the mean squared error minimization problem $\arg\min_{\mathbf{W}} E\{\|\mathbf{S} - \mathbf{W}\hat{\mathbf{Y}}\|^2\}$ leads to the well known filter matrix:

$$\mathbf{W} = (\mathbf{\Phi}_{\mathbf{SS}}^{-1} + \mathbf{H}^H \mathbf{\Phi}_{\boldsymbol{\epsilon\epsilon}}^{-1} \mathbf{H})^{-1} \mathbf{H}^H \mathbf{\Phi}_{\boldsymbol{\epsilon\epsilon}}^{-1}. \tag{9}$$

Since the filter matrix is not bias anymore one can overcome this problem by modifying the filter by a diagonal matrix that restores unit gain, leading to a new filter matrix given as $\mathbf{W}_{UB} = \operatorname{diag}\left(\operatorname{diag}^{-1}(\mathbf{W} \cdot \mathbf{H})\right) \cdot \mathbf{W}$. The SINR per antenna is is given as the diagonal elements of the error covariance matrix,

$$\gamma_{tx} = \frac{1}{[(\mathbf{\Phi_{SS}} + \mathbf{H}^H \mathbf{\Phi}_{\boldsymbol{\epsilon\epsilon}}^{-1} \mathbf{H})^{-1} \mathbf{\Phi}_{\mathbf{SS}}^{-1}]_{tx,tx}} - 1. \tag{10}$$

3.2. Parallel Interference Cancellation, PIC

The idea in the case of a Parallel Interference Cancellation scheme is to split the MIMO detection problem into several SIMO detection problems and therefore take advantage of receive diversity [9]. This is done by subtracting soft remodulated symbols $\hat{S}_{tx}$ form the received signal (see [8] for details) and thus cancelling out the interference caused by other transmit antennas. Furthermore the following more general expectations as presented in [10] are used which are also applicable for QAM modulation: $E\{S_{tx}S_{tx}^*\} = \sigma^2_{S_{tx}}$ and $E\{\hat{S}_{tx}S_{tx}^*\} = E\{S_{tx}\hat{S}_{tx}^*\} = E\{\hat{S}_{tx}\hat{S}_{tx}^*\} = \sigma^2_{S_{tx}}(1-\vartheta_{tx})$, with $\vartheta_{tx} = Var\{\hat{S}_{tx}\}$ (variance of estimated symbols) and $\boldsymbol{\vartheta} = \operatorname{diag}(\vartheta_{tx})$. In order to find the optimal filter matrix for antenna tx according to the MMSE criterion one has to minimize the following cost function $\arg\min_{\mathbf{W}_{tx}} E\{\|S_{tx} - \mathbf{W}_{tx}(\hat{\mathbf{Y}}' + \mathbf{H}_{(:,tx)}\hat{S}_{tx})\|^2\}$ given $\hat{\mathbf{Y}}' = \hat{\mathbf{Y}} - \mathbf{H}\hat{\mathbf{S}}$. Finally the filter matrix per transmit antenna is given as:

$$G_{tx} = \sigma^2_{tx}\mathbf{H}^H_{(:,tx)}[\underbrace{\mathbf{H}(\mathbf{\Phi_{SS}}\boldsymbol{\vartheta})\mathbf{H}^H + \mathbf{\Phi_{\epsilon\epsilon}}}_{\mathbf{\Lambda}} + \mathbf{H}_{(:,tx)}\sigma^2_{tx}(1-\vartheta_{tx})\mathbf{H}^H_{(:,tx)}]^{-1} \tag{11}$$

with $\mathbf{\Lambda}$ as an error term consisting of remaining multiple antenna interference, AWGN noise and remaining ICI noise. The SINR is now given as:

$$\gamma_{tx} = \frac{1}{1 - \sigma^2_{tx}\mathbf{H}^H_{(:,tx)}[\mathbf{\Lambda} + \mathbf{H}_{(:,tx)}\sigma^2_{tx}(1-\vartheta_{tx})\mathbf{H}^H_{(:,tx)}]^{-1}\mathbf{H}_{(:,tx)}} - 1. \tag{12}$$

3.3. Successive Interference Cancellation, SIC

The SIC technique is based on a decomposition of the channel matrix $\mathbf{H}$ such that the currently detected symbol depends only on previously detected signals. It is obviously advantageous to detect the strongest antenna first, in order to minimize the effects of error propagation. For this purpose we use the MMSE based sorted $\mathbf{QR}$ decomposition introduced in [11] which we extended to a more general approach. The Euclidian distance computation after applying a whitening filter and extension to MMSE is given as:

$$\left\| \begin{bmatrix} \mathbf{\Phi}_{\boldsymbol{\epsilon\epsilon}}^{-\frac{1}{2}}\hat{\mathbf{Y}} \\ \mathbf{0} \end{bmatrix} - \left(\begin{bmatrix} \mathbf{\Phi}_{\boldsymbol{\epsilon\epsilon}}^{-\frac{1}{2}}\mathbf{H} \\ \mathbf{\Phi}_{\mathbf{SS}}^{-\frac{1}{2}} \end{bmatrix} - \begin{bmatrix} \mathbf{0} \\ \mathbf{\Phi}_{\mathbf{SS}}^{-\frac{1}{2}} \end{bmatrix} \right) \mathbf{S} \right\|^2 \tag{13}$$

applying the decomposition to $\begin{bmatrix} \mathbf{\Phi}_{\boldsymbol{\epsilon\epsilon}}^{-\frac{1}{2}}\mathbf{H} \\ \mathbf{\Phi}_{\mathbf{SS}}^{-\frac{1}{2}} \end{bmatrix} = \begin{bmatrix} \mathbf{Q}_1 \\ \mathbf{Q}_2 \end{bmatrix} \mathbf{R}$ and multiplication with $\mathbf{Q}^H$ leads to the following expression

$$\left\| \mathbf{Q}_1^H \mathbf{\Phi}_{\boldsymbol{\epsilon\epsilon}}^{-\frac{1}{2}}\hat{\mathbf{Y}} - \underbrace{(\mathbf{R} - \operatorname{diag}(\mathbf{Q}_2^H)\mathbf{\Phi}_{\mathbf{SS}}^{-\frac{1}{2}})}_{\mathbf{R}_{UB}} \hat{\mathbf{S}} + \overline{\operatorname{diag}}(\mathbf{Q}_2^H)\mathbf{\Phi}_{\mathbf{SS}}^{-\frac{1}{2}}\mathbf{S} \right\|^2 \tag{14}$$

where we replaced $\mathbf{S}$ in the second term by its soft representation $\hat{\mathbf{S}}$. If $\mathbf{R}_{UB}$ is used instead of $\mathbf{R}$ the initially introduced Bias is considered and an unbiased MMSE-SIC is implemented. However, $\overline{\mathrm{diag}}(\mathbf{Q}_2^H)$ is a strong lower triangular matrix and is coupled in the SIC with *non* detected symbols. This Bias term cannot be removed and reflects the trade off between interference suppression and noise enhancement. Finally the SINR is given as:

$$\gamma_{tx} = \frac{\sigma_{tx}^2}{[\mathbf{I} + \mathbf{R}_{UB} Var\{\hat{\mathbf{S}}\} + \overline{\mathrm{diag}}(\mathbf{Q}_2^H)\overline{\mathrm{diag}}(\mathbf{Q}_2)]_{tx,tx}}. \quad (15)$$

4. NUMERICAL RESULTS

The performance of the presented receiver schemes was tested by simulating a 4×4 MIMO system with $N_C = 64$ carriers including 4 pilots and 12 zero carries (IEEE 802.11a),16-QAM. As for the channel we selected an IEEE 802.11n E channel. A rate 1/2 convolution code with $G = [133, 171]_8$ was chosen as channel code. Fig. 2 shows the frame error rate (FER)

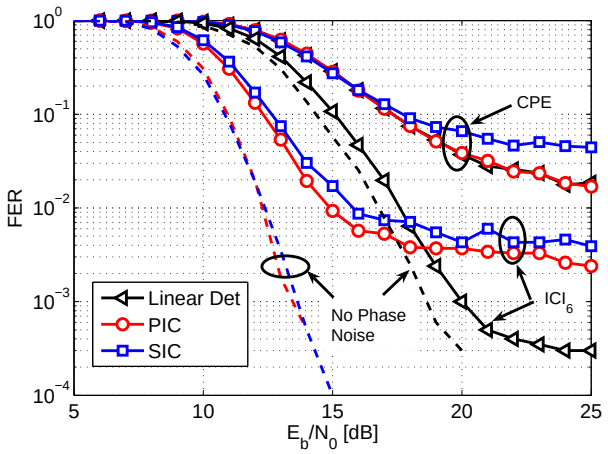

Fig. 2. Performance of iterative PN correction up to order $u = 6$ (4×4 MIMO, $N_C = 64$, 16-QAM, $\delta_{3dB} = 0.01$)

for different detection schemes and correction orders for an oscillator quality of $\delta_{3dB} = 0.01$. Looking at the no PN performance (dashed curves) the cancellation techniques outperform the linear detection (LD) by more than 5dB. Under the presence of PN and only CPE correction (1st iteration) the LD and the PIC result in the same behavior whereas the SIC performs worse. If the mitigation of higher PN components is enabled, the BER of the cancellation schemes decays earlier than the LD. However, a crossing point at high SNR is observed. We are discussing 2 possible explanation of this behavior. The first one is error propagation during the cancellation step, noticeable in the higher CPE error floor of the SIC. The second is the impact of the non Gaussian distribution of the remaining ICI. Looking at high SNR the AWGN noise is not the dominant error term anymore. Additionally assuming perfect multiple antenna interference (MAI) cancellation leaves the remaining ICI as the dominant term. Since the ICI distribution is non Gaussian (Fig. 3) the Euclidian distance

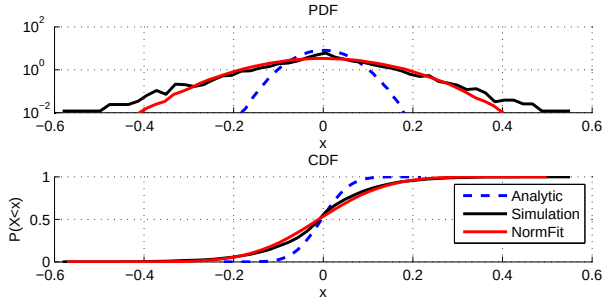

Fig. 3. ICI distribution after PN estimation up to order $u = 2$

computation (Eq. (8)) is not the correct representation of the L-values which would be a ratio of the true probability. However, the true representation is currently not analytically feasible. This is not the case in LD where the MAI is not cancelled out in advance and thus still leading to a valid Gaussian error approximation. The distribution of the ICI is given in Fig 3. Here the "Analytic" plot shows the common Gaussian assumption for a relative oscillator linewidth of $\delta_{3dB} = 0.01$ which does not take into account the heavy tail probability of the ICI PN components ("Simulation" plot). Since we cannot express the analytic distribution of the ICI we applied a normal distribution fitting on the simulated data obtaining a new variance ("NormFit" plot). The SNR and oscillator linewidth independent scaling factors between the analytic and NormFit data are given in the following Table.

Iteration	1 (CPE)	2	3	4	5	6	7
Factor	1.9	3.9	5.7	7.2	8.6	9.8	10.8

One way to further describe the properties of a probability distribution is the so called kurtosis. The kurtosis is defined as the fourth moment about the mean divided by the square of the variance of the probability distribution. A gaussian distribution has got a kurtosis of 3. Fig. 4 shows the kurtosis over different oscillator linewidths for the CPE correction and for the ICI correction up to an order of $u = 2$. At low δ_{3dB} the kurtosis is bigger than 3. Such a leptokurtic distribution has a more acute peak and long tails giving a higher probability than a normal distributed variable of fast phase noise variations. At high δ_{3dB} the kurtosis is much below 3. Such a platykurtic distribution is associated with a smaller peak around the mean and thin tails. This results of lower probability than a gaussian distribution of values close to the mean. Thus the remaining ICI distribution can never be considered as gaussian distributed.

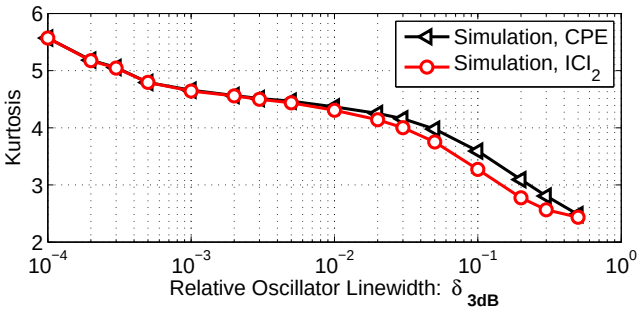

Fig. 4. Kurtosis for different oscillator linewidths

Therefore, we applied the factors given in table above to modify the remaining ICI variance term and investigated the genie PIC behavior where the MAI is cancelled out perfectly. The results are presented in Fig 5. The genie PIC was chosen

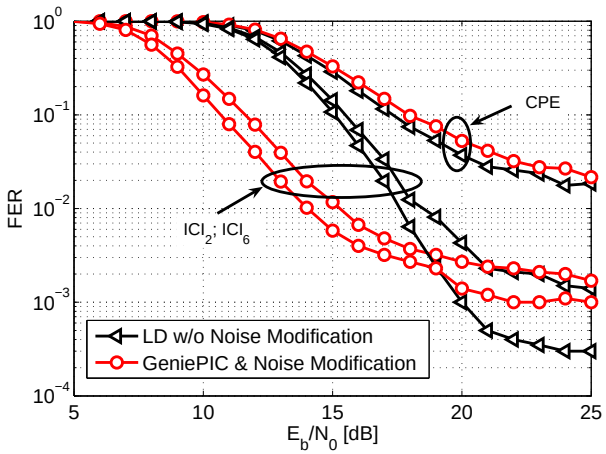

Fig. 5. Genie PCI, setup as given in Fig. 2

to show that the remaining error floor is not mainly caused by error propagation in the cancellation step. It can be seen from the figure that crossing points for $u = \{2, 6\}$ are still existing. Hence, the impact of the non Gaussian distribution could be reduced by considering the tail probability and disregarding the center probability. However, looking at the CPE correction the result is even worse. Thus we further investigate the statistics of the remaining ICI by performing Kolmogorov-Smirnov tests in such a way that the null hypothesis is that the values come from a normal distribution. The decision to reject the null hypothesis occurs when the significance level equals or exceeds the so called p-value. In Fig. 6 the p-values are plotted for different oscillator linewidths. The curve "Simulation, CPE" represents the p-value of the remaining ICI without noise modification. The curve lies above the "NormFit, CPE" curve at $\delta_{3dB} = 0.01$ which implies that applying a fitting at the first iteration leads to an even less Gaussian distribution and thus performance degradation (Fig 5). How-

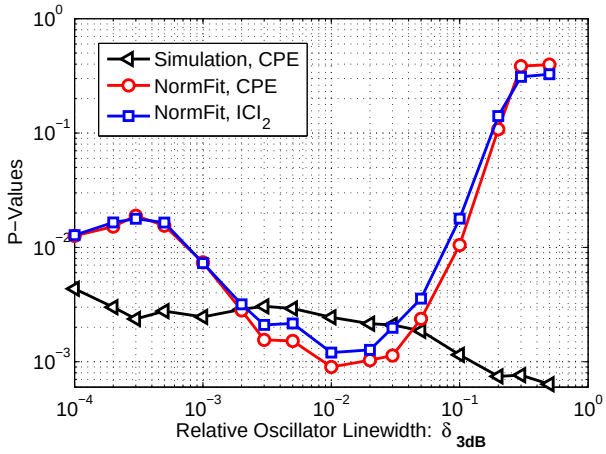

Fig. 6. Gaussian test of remaining ICI

ever, for every further iteration the "Simulation" curves (not shown since too low) are lying much lower than the "NormFit" curves. Finally the SIC and PIC behavior with optimal

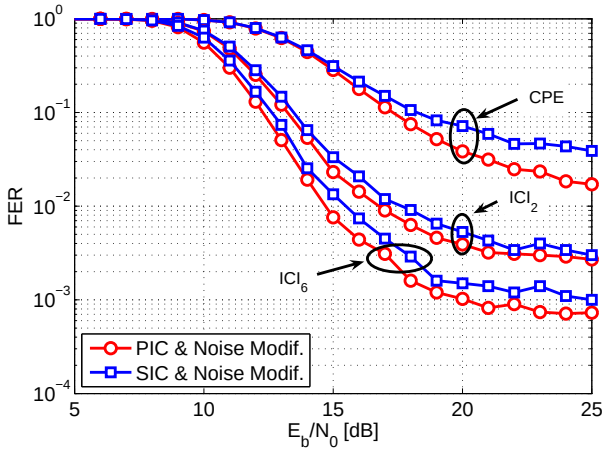

Fig. 7. ICI noise modification, setup as Fig. 2

scaling factors is shown in Fig 7 indicating an improvement compared to Fig 2.

5. CONCLUSIONS

In this work we discussed the performance of different iterative MIMO-OFDM schemes under the presence of PN. We emphasized the importance of taking the non Gaussian distribution of the PN ICI noise into account in the calculation of the detector soft output. The lowest error floor was achieved by using a linear filter. This is due to the fact that the superposition of multiple antenna interference and ICI leads to a Gaussian distribution of the noise at the filter output. For interference cancellation techniques, in contrast, the main source of noise in the high SNR regime is the non Gaussian

distributed ICI, which leads to a non optimal soft output and thus higher error floors. We were able to overcome this problem by calculating a modified noise variance based on a fitting of the distribution of the remaining ICI to a normal distribution. An alternative to even further lower the error floor is the use of stronger codes.

6. REFERENCES

[1] D. Petrovic, W. Rave, and G. Fettweis, "Phase Noise Suppression in OFDM Including Intercarrier Interference," in *InOWo*, 2003.

[2] S. Wu, P Liu, and Y. Bar-Ness, "Phase Noise Estimation and Mitigation for OFDM Systems," *IEEE Transactions on Wireless Communications*, vol. 5, no. 12, pp. 3616–3625, 2006.

[3] T. C. W. Schenk, X.-J. Tao, P. F. M. Smulders, and E. R. Fledderus, "Influence and Suppression of Phase Noise in Multi-Antenna OFDM," in *IEEE Vehicular Technology Conference (VTC)*, 2004.

[4] S. Bittner, W. Rave, and G. Fettweis, "Phase Noise Suppression in OFDM with Spatial Multiplexing," in *IEEE Vehicular Technology Conference (VTC)*, 2007, (accepted for publication).

[5] T. C. W. Schenk, X.-J. Tao, P. F. M. Smulders, and E. R. Fledderus, "On the Influence of Phase Noise Induced ICI in MIMO OFDM Systems," *IEEE Communications Letters*, vol. 9, no. 8, pp. 682–684, 2005.

[6] A. Demir, A. Mehrotra, and J. Roychowdhury, "Phase Noise in Oscillators: A Unifying Theory and Numerical Methods for Characterisation," *IEEE Transactions on Circuits and Systems—Part I: Fundamental Theory and Applications*, vol. 47, no. 5, pp. 655–674, 2000.

[7] D. Petrovic and G. Fettweis W. Rave, "Intercarrier Interference due to Phase Noise in OFDM: Estimation and Suppression," in *IEEE Vehicular Technology Conference (VTC)*, 2004.

[8] S. Bittner, E. Zimmermann, and G. Fettweis, "Low Complexity Soft Interference Cancellation for MIMO-Systems," in *IEEE Vehicular Technology Conference (VTC)*, 2006.

[9] H. Lee, B. Lee, and I. Lee, "Iterative Detection and Decoding With an Improved V-BLAST for MIMO-OFDM Systems," *IEEE Journal on Selected Areas in Communications*, vol. 24, no. 3, pp. 504–513, 2006.

[10] R. Wohlgenannt, K. Kansanen, D. Tujkovic, and T. Matsumoto, "Outage-based LDPC Code Design for SC/MMSE Turbo-Equalization," in *IEEE Vehicular Technology Conference (VTC)*, 2005.

[11] D. Wübben, R. Böhnke, V. Kühn, and K. D. Kammeyer, "MMSE Extension of V-BLAST based on Sorted QR Decomposition," in *IEEE Vehicular Technology Conference (VTC)*, 2003.